Fermi National Accelerator Laboratory

FN-546

Evaluation of Wake Forces in a Dielectric-Lined Waveguide

King-Yuen Ng
Fermi National Accelerator Laboratory
P.O. Box 500
Batavia, Illinois 60510

July 1990

Operated by Universities Research Association Inc. under contract with the United States Department of Energy

FN-546

EVALUATION OF WAKE FORCES IN A DIELECTRIC-LINED WAVEGUIDE

King-Yuen Ng

Fermi National Accelerator Laboratory Batavia, IL 60510*

(July 1990)

ABSTRACT

The longitudinal and transverse wake forces in a dielectric-lined waveguide are evaluated numerically. Analytic expressions are given for the special cases when the dielectric is thin and thick. The results are compared with the wake forces in an iris-loaded waveguide.

(A combination of this note and FN-533 has been accepted for publication in Physical Review D.)

*Operated by the Universities Research Association, Inc., under contracts with the U.S. Department of Energy.

I. INTRODUCTION

Wake field accelerators[1,2,3] are of great interest because of their potential for providing very high acceleration gradients for the next generation of accelerators. They will be of more interest if the transverse wake force is small enough so that beam breakup[4] will no longer pose a problem. In Ref. 5, we considered a waveguide consisting of a cylindrical metallic tube of radius a with infinite wall conductivity and filled partially with an isotropic material of dielectric constant ϵ between radii $b < r < a$. We showed vigorously that the transverse wake force does not vanish even when v, the velocity of the source particle, approaches c, the velocity of light. However, it was shown experimentally[6] that transverse deflections appeared to be much smaller in dielectric-lined waveguides than in structured-waveguides and plasma-waveguides.[7,8] It is therefore of great interest to evaluate the longitudinal and transverse wake forces in the dielectric waveguide, so that comparison can be made with other wake-field devices.

II. SOME FORMULAS

Consider a source particle carrying charge q travels with velocity $v = \beta c$ along the cylindrical dielectric-loaded waveguide at an offset r_0 from its axis. A test particle carrying charge e travels at the same velocity lagging at a distance z behind and at an offset r. The $m = 0$ longitudinal force on the test particle can be written, according to Eq. (3.9) of Ref. 5, as

$$F_{z0}(z) = -\frac{eq}{a^2} \sum_{\lambda} \hat{F}_{z0\lambda}(x_{0\lambda}) \cos \frac{x_{0\lambda} z}{a\sqrt{\epsilon - 1}} , \tag{2.1}$$

where

$$\hat{F}_{z0\lambda} = \frac{4}{\epsilon \xi} \frac{x_{0\lambda} p_0(x_{0\lambda})}{\mathcal{D}_0'(x_{0\lambda})} , \tag{2.2}$$

$x_{0\lambda}$ is the λ-th *positive* zero of $\mathcal{D}_0$, and $\xi = b/a$ is the ratio of the inner radius to the outer radius of the dielectric. Similarly, with the aid of Eq. (4.7) of Ref. 5 and Panofsky's theorem,[9] the $m \geq 1$ transverse force can be written as

$$F_{rm}(r, z; r_0) = \frac{eq}{a^2} \left(\frac{r_0}{a}\right)^m \left(\frac{r}{a}\right)^{m-1} \sum_{\lambda} \hat{F}_{rm\lambda}(x_{m\lambda}) \sin \frac{x_{m\lambda} z}{a\sqrt{\epsilon - 1}} , \tag{2.3}$$

where

$$\hat{F}_{rm\lambda} = \frac{8m\sqrt{\epsilon - 1}}{\xi^{2m}} \frac{p_m(x_{m\lambda}) r_m(x_{m\lambda})}{\mathcal{D}_m'(x_{m\lambda})} , \tag{2.4}$$

and $x_{m\lambda}$ is the λ-th *positive* zero of $\mathcal{D}_m$. In the above, the analytic functions $\mathcal{D}_0$ and $\mathcal{D}_m$ are given by

$$\mathcal{D}_0(x) = xp_0' + \frac{x^2\xi}{2\epsilon}p_0 \ , \tag{2.5}$$

$$\mathcal{D}_m(x) = \left[\frac{x^2\xi^2}{m+1} - m(\mu\epsilon+1)\right] p_m r_m + x\xi[\epsilon p_m' r_m + \mu r_m' p_m] \qquad m \neq 0 \ . \tag{2.6}$$

For simplicity, the relative magnetic permeability μ of the dielectric has been put equal to unity. The cross-products of Bessel functions in Eqs. (2.5) and (2.6) are defined as

$$\begin{aligned} p_m(x) &= J_m(x)Y_m(x\xi) - Y_m(x)J_m(x\xi) \ , \\ r_m(x) &= J_m'(x)Y_m(x\xi) - Y_m'(x)J_m(x\xi) \ , \\ p_m'(x) &= J_m(x)Y_m'(x\xi) - Y_m(x)J_m'(x\xi) \ , \\ r_m'(x) &= J_m'(x)Y_m'(x\xi) - Y_m'(x)J_m'(x\xi) \ . \end{aligned} \tag{2.7}$$

In the event that $\mathcal{D}_0(x)$ $[\mathcal{D}_m(x)]$ is not analytic, it can be made analytic by multiplication of x to an appropriate power. Needless to say, we have to multiply the numerator of Eq. (2.2) [Eq. (2.4)] by the same power of x.

In below, the dimensionless *reduced* wake forces $\hat{F}_{z0\lambda}$ and $\hat{F}_{rm\lambda}$ will be evaluated. The zeroes $x_{0\lambda}$ and $x_{m\lambda}$ are dimensionless *reduced* eigen frequencies of the eigen modes. The true eigen frequencies are given by $\omega_{m\lambda} = x_{m\lambda}c/a\sqrt{\epsilon-1}$.

III. THIN DIELECTRIC LINING

Let $a\delta$ denote the thickness of the dielectric lining; or $\delta = 1 - \xi$. Here we consider the situation of a thin lining; i.e., $\delta \ll 1$. In Eq. (2.7), p_m, p_m', r_m, and r_m' are defined as functions of $x = sa$ and $x\xi = sb = x - x\delta$. When $x\delta \ll 1$, we Taylor expand them up to δ. With the aid of the wronskian of J_m and Y_m as well as the Bessel equation, we obtain

$$\begin{aligned} p_m(x) &= -\frac{2\delta}{\pi} \\ p_m'(x) &= \frac{2(1+\delta)}{\pi x} \\ r_m(x) &= -\frac{2}{\pi x} \end{aligned}$$

$$r'_m(x) = -\frac{2\delta}{\pi}\left(1 - \frac{m^2}{x^2}\right) . \tag{3.1}$$

Thus, retaining only the lowest order of δ,

$$\mathcal{D}_0(x) = \frac{2}{\pi} - \frac{x^2\delta}{\pi\epsilon} , \tag{3.2}$$

and for $m \neq 0$,

$$x\mathcal{D}_m(x) = \frac{4\delta}{\pi^2}\left[\frac{x^2}{m+1} - \frac{\epsilon}{\delta}\right] . \tag{3.3}$$

We see that there is only one positive zero in Eq. (3.2) or (3.3), namely,

$$\begin{aligned} x_{01} &= \sqrt{\frac{2\epsilon}{\delta}} \\ x_{m1} &= \sqrt{\frac{(m+1)\epsilon}{\delta}} \qquad m \neq 0 . \end{aligned} \tag{3.4}$$

This justifies the approximation used to obtain Eqs. (3.1); i.e., $x\delta \ll 1$ when the dielectric is sufficiently thin. The eigen frequency happens to be the same for the $m = 0$ and $m = 1$ modes. One can compute easily the reduced wake forces,

$$\hat{F}_{z01} = 4 , \tag{3.5}$$

$$\hat{F}_{rm1} = 4m\sqrt{\frac{(\epsilon-1)(m+1)\delta}{\epsilon}} . \tag{3.6}$$

The ratio of the reduced forces are

$$\frac{\hat{F}_{rm1}}{\hat{F}_{z01}} = m\sqrt{m+1}\sqrt{\frac{(\epsilon-1)\delta}{\epsilon}} . \tag{3.7}$$

The behavior of the limit $\delta \to 0$ is not intuitive. As $\delta \to 0$, one expects the absence of the dielectric lining leaving behind a perfectly conducting pipe wall. The electromagnetic fields generated by source particle are therefore just the ordinary space-charge fields, which we have omitted after setting $\gamma \to \infty$. However, the longitudinal wake force as shown by Eq. (3.5) does not vanish as $\delta \to 0$. Thus, an infinitely thin dielectric lining does not imply no dielectric lining. Our evaluation of the wake forces here bases on Eqs. (2.1) and (2.3), where $\gamma \gg \omega a/c$ is assumed. With the substitution of Eq. (3.4), this assumption becomes $\gamma \gg \sqrt{2\epsilon/\delta(\epsilon-1)}$. As a result, our calculation cannot lead to the situation of $\delta = 0$, or the removal of the dielectric lining.

IV. THICK DIELECTRIC LINING

Here, we consider the situation when the inner radius of the dielectric $b = a\xi$ approaches zero. Assuming that $x\xi \ll 1$, we use the large-argument expansions of Bessel functions to obtain

$$\begin{aligned} p_0(x) &= \frac{2}{\pi}\left(\ln\frac{x\xi}{2} + \epsilon\right) J_0(x) - Y_0(x) \,, \\ p_0'(x) &= \frac{2}{\pi x\xi} J_0(x) + \frac{x\xi}{2} Y_0(x) \,, \end{aligned} \tag{4.1}$$

where $\epsilon = 0.57722$ is an Euler number. Retaining only the lowest order in $x\xi$, we get

$$\mathcal{D}_0(x) = \frac{2}{\pi\xi} J_0(x) + \frac{x^2\xi(\epsilon-1)}{2\epsilon} \,. \tag{4.2}$$

Since $x\xi \ll 1$, the λ-th zero $x_{0\lambda}$ of $\mathcal{D}_0$ should be very close to the λ-th zero $\bar{x}_{0\lambda}$ of J_0. If we write

$$x_{0\lambda} = \bar{x}_{0\lambda} + \Delta_{0\lambda} \,, \tag{4.3}$$

$$J_0(x_{0\lambda}) \approx \Delta_{0\lambda} J_0'(\bar{x}_{0\lambda}) = -\Delta_{0\lambda} J_1(\bar{x}_{0\lambda}) \,. \tag{4.4}$$

We can then solve from Eq. (4.2) the λ-th zero of $\mathcal{D}_0$,

$$x_{0\lambda} = \bar{x}_{0\lambda} + \frac{\pi(\epsilon-1)}{\epsilon}\left(\frac{x\xi}{2}\right)^2 \frac{Y_0(\bar{x}_{0\lambda})}{J_1(\bar{x}_{0\lambda})} \,. \tag{4.5}$$

The corresponding $m = 0$ reduced longitudinal wake force becomes

$$\hat{F}_{z0\lambda} = \frac{2\pi\bar{x}_{0\lambda}}{\epsilon}\frac{Y_0(\bar{x}_{0\lambda})}{J_1(\bar{x}_{0\lambda})} \,. \tag{4.6}$$

We see that the eigen frequencies approach those of the $\mathrm{TM}_{0\lambda}$ modes in a cylindrical dielectric-filled waveguide. In fact, this is to be expected because the dielectric becomes filling the whole waveguide when $\xi \to 0$.

The higher-order reduced forces can be computed similarly. With $x\xi \ll 1$ and $m \neq 0$,

$$p_m(x) = -\frac{(m-1)!}{\pi}\left(\frac{2}{x\xi}\right)^m \left[J_m(x) + \frac{\pi}{m!(m-1)!}\left(\frac{xt}{2}\right)^{2m} Y_m(x)\right] \,,$$

$$
\begin{aligned}
p'_m(x) &= \frac{m!}{\pi x\xi}\left(\frac{2}{x\xi}\right)^m\left[J_m(x) - \frac{\pi}{m!(m-1)!}\left(\frac{xt}{2}\right)^{2m}Y_m(x)\right] , \\
r_m(x) &= -\frac{(m-1)!}{\pi}\left(\frac{2}{x\xi}\right)^m\left[J'_m(x) + \frac{\pi}{m!(m-1)!}\left(\frac{xt}{2}\right)^{2m}Y'_m(x)\right] , \\
r'_m(x) &= \frac{m!}{\pi x\xi}\left(\frac{2}{x\xi}\right)^m\left[J'_m(x) - \frac{\pi}{m!(m-1)!}\left(\frac{xt}{2}\right)^{2m}Y'_m(x)\right] . \qquad (4.7)
\end{aligned}
$$

If the terms involving Y_m and Y'_m are neglected as we take the limit $x\xi \to 0$, it is easy to see that

$$\mathcal{D}_m(x) \propto J_m(x)J'_m(x) . \qquad (4.8)$$

Thus, the eigen modes are characterized by $\bar{x}_{m\lambda}$, the λ-th zero of J_m, and $\bar{x}'_{m\lambda}$, the λ-th zero of J'_m. However, the reduced transverse force $\hat{F}_{rm\lambda}$ which is proportional to $p_m r_m$ as depicted by Eq. (2.4) will vanish identically. As a result, we must compute the zeroes of $\mathcal{D}_m(x)$ to the next order in $x\xi$. Denote the two series of zeroes by

$$
\begin{aligned}
x_{m\lambda} &= \bar{x}_{m\lambda} + \Delta_{m\lambda} , \qquad (4.9) \\
x'_{m\lambda} &= \bar{x}'_{m\lambda} + \Delta'_{m\lambda} . \qquad (4.10)
\end{aligned}
$$

Near the zeroes of $x_{m\lambda}$, we have

$$\mathcal{D}_m(x) = -\frac{2m!(m-1)!}{\pi^2}\left(\frac{2}{x\xi}\right)^{2m}J'_m(x)\left[(\epsilon+1)J_m(x) + \frac{\pi}{m!(m-1)!}\left(\frac{x\xi}{2}\right)^{2m}Y_m(x)\right] . \qquad (4.11)$$

We expand $J_m(x)$ near $\bar{x}_{m\lambda}$ to obtain

$$J_m(x_{m\lambda}) \approx \Delta_{m\lambda}J'_m(\bar{x}_{m\lambda}) , \qquad (4.12)$$

and solve Eq. (4.11) to get

$$\Delta_{m\lambda} = -\frac{1}{\epsilon+1}\frac{\pi}{m!(m-1)!}\left(\frac{\bar{x}_{m\lambda}\xi}{2}\right)^{2m}\frac{Y_m(\bar{x}_{m\lambda})}{J'_m(\bar{x}_{m\lambda})} . \qquad (4.13)$$

We are now able to compute up to the next order of $x\xi$,

$$p_m(x_{m\lambda})r_m(x_{m\lambda}) = -\frac{\epsilon}{\epsilon+1}\frac{1}{m\pi}J'_m(\bar{x}_{m\lambda})Y_m(\bar{x}_{m\lambda}) , \qquad (4.14)$$

and arrive at the corresponding reduced transverse force

$$\hat{F}_{rm\lambda} = \frac{\epsilon\sqrt{\epsilon-1}}{(\epsilon+1)^2}\frac{4\pi}{m!(m-1)!}\left(\frac{\bar{x}_{m\lambda}}{2}\right)^{2m}\frac{Y_m(\bar{x}_{m\lambda})}{J'_m(\bar{x}_{m\lambda})} \ . \tag{4.15}$$

Near the zeroes $x'_{m\lambda}$, we have

$$\mathcal{D}_m(x) = -\frac{2m!(m-1)!}{\pi^2}\left(\frac{2}{x\xi}\right)^{2m} J_m(x)\left[(\epsilon+1)J'_m(x) + \frac{\epsilon\pi}{m!(m-1)!}\left(\frac{x\xi}{2}\right)^{2m} Y'_m(x)\right] \ . \tag{4.16}$$

Since

$$J'_m(x'_{m\lambda}) \approx \Delta J''_m(\bar{x}'_{m\lambda}) = -\Delta_{m\lambda}\left(1-\frac{m^2}{\bar{x}'^2_{m\lambda}}\right)J_m(\bar{x}'_{m\lambda}) \ , \tag{4.17}$$

we obtain

$$\Delta'_{m\lambda} = \frac{\epsilon}{\epsilon+1}\frac{\pi}{m!(m-1)!}\frac{1}{1-m^2/\bar{x}'^2_{m\lambda}}\left(\frac{\bar{x}'_{m\lambda}\xi}{2}\right)^{2m}\frac{Y'_m(\bar{x}'_{m\lambda})}{J_m(\bar{x}'_{m\lambda})} \ . \tag{4.18}$$

Now we can compute up to the next order of $x\xi$

$$p_m(x'_{m\lambda})r_m(x'_{m\lambda}) = \frac{1}{\epsilon+1}\frac{1}{m\pi}J_m(\bar{x}'_{m\lambda})Y'_m(\bar{x}'_{m\lambda}) \ . \tag{4.19}$$

and arrive at the corresponding reduced transverse force

$$\hat{F}'_{rm\lambda} = \frac{\sqrt{\epsilon-1}}{(\epsilon+1)^2}\frac{4\pi}{m!(m-1)!}\left(\frac{\bar{x}'_{m\lambda}}{2}\right)^{2m}\frac{1}{1-m^2/\bar{x}'^2_{m\lambda}}\frac{Y'_m(\bar{x}'_{m\lambda})}{J_m(\bar{x}'_{m\lambda})} \ . \tag{4.20}$$

As expected, when $\xi \to 0$, the two series of reduced eigen frequencies $x_{m\lambda}$ and $x'_{m\lambda}$ ($m \neq 0$) correspond to the $\mathrm{TM}_{m\lambda}$ and $\mathrm{TE}_{m\lambda}$ modes in a cylindrical dielectric-filled waveguide. In the present dielectric-lined waveguide, the modes are hybrid and are referred to as $\mathrm{HM}_{m\lambda}$ and $\mathrm{HE}_{m\lambda}$ instead. The lowest mode at $\xi = 0$ is the HE_{11} mode, with $x'_{11} = 1.8411$, which is lower than the lowest longitudinal HM_{01} mode with $x_{01} = 2.405$. The lowest transverse HM mode at $\xi = 0$ is $x_{11} = 3.8171$.

V. NUMERICAL EVALUATION

The wake forces corresponding to thin-dielectric and thick-dielectric limits have been evaluated analytically. In between, no simple analytic formulas are possible and

numerical evaluation is necessary. The zeroes of $\mathcal{D}_0$ and $\mathcal{D}_m$ are first located and the summations in Eqs. (2.1) and (2.3) are performed term by term.

Experimentally, the source is not a single particle but a source bunch of total charge q having a rms longitudinal length σ_ℓ. If the center of the bunch travels according to $z = ct$ and the longitudinal charge distribution is gaussian, the wakes left behind are again given by Eq. (2.1) and (2.3) with each term in the summand multiplied, in the limit $\beta \to 1$, by

$$\exp\left[-\frac{1}{2}\left(\frac{x_\lambda \sigma_\ell}{a\sqrt{\mu\epsilon-1}}\right)^2\right] . \tag{5.1}$$

Since σ_ℓ is finite, consequently only the first few characteristic waves will contribute significantly. For the sake of clarity, we shall restrict ourselves to the lowest mode in the following discussion.

The reduced eigen frequencies corresponding to the lowest $m = 0$ longitudinal mode x_{01} (TM_{01}) and lowest $m = 1$ transverse mode x'_{11} (HE_{11}) are shown, respectively, in Figs. 1 and 2 for ξ ranging from 0 to 1, with dielectric constant $\epsilon = 1.2$, 2.0, 3.0, and 4.0. The ratio of the two lowest eigen frequencies is displayed in Fig. 3. In general, larger dielectric constant leads to higher eigen frequencies. The lowest reduced eigen frequencies for the monopole and dipole modes start off from, respectively, $x_{01} = 2.405$ and $x'_{11} = 1.841$ at $\xi = 0$, increase rather slowly with ξ when $\xi \lesssim 0.5$, but increase rapidly to infinity according to Eq. (3.4) afterward.

The reduced ($m = 0$) longitudinal and ($m = 1$) wake forces of the lowest modes, $\hat{F}_{z01}$ and $\hat{F}'_{r11}$, are shown, respectively, in Figs. 4 and 5, and their ratio in Fig. 6. We see that the reduced transverse force as well as the ratio of transverse to longitudinal forces start off almost constant at $\xi \sim 1$ and increase rather slowly with larger ξ. They vanish rapidly only when ξ is sufficiently close to 1; or when the dielectric lining is sufficiently thin. However, $\xi \approx 1$ is not a good region to operate a wakefield accelerator. The wake fields are generated by Cerenkov radiation inside the dielectric, and when the dielectric lining is thin, such radiation is minimal. In addition, the wake field wavelength will be too short to work with. This is seen by examining the cosine factor in Eq. (2.1) with an extremely high reduced eigen frequency ($\sim \delta^{-1/2}$) as depicted in Eq. (3.4) and Fig. 1. To avoid large transverse forces, the other option appears to be the sector of small ξ. This is the configuration of thick dielectric lining. For this reason, the analytic formulas developed for thick dielectric lining are very good approximation in practice. In this

region, the reduced transverse wake force $\hat{F}'_{r11}$ depends on the dielectric constant mainly through the factor $\sqrt{\epsilon-1}/(\epsilon+1)^2$ and weakly through x'_{11}, as indicated by Eq. (4.20). Consequently, we see (also in Fig. 2) $\hat{F}'_{r11}$ reach a maximum at $\epsilon \approx 5/3$, and decrease at larger ϵ. However, $\hat{F}_{z01}$ decreases with dielectric constant as $1/\epsilon$ as depicted in Eq. (4.6) and Fig. 1. The result is that the ratio $\hat{F}'_{r11}/\hat{F}_{z01}$ decreases with ϵ (when $\epsilon > 1$). Therefore, to reduce $\hat{F}'_{r11}$ as well as $\hat{F}'_{r11}/\hat{F}_{z01}$, a large ϵ is favored.

As an illustration, let us consider a cylindrical waveguide with outer radius $a = 1$ cm lined with a material having a dielectric constant $\epsilon = 3$. The thickness of the material is taken as $a-b = 0.8$ cm, or $\xi = 0.2$. The lowest reduced eigen frequencies are $x_{01} = 2.518$ for $m = 0$ and $x_{11} = 1.954$ for $m = 1$. They correspond to frequencies $\omega_{01}/2\pi = 8.496$ GHz and $\omega_{11}/2\pi = 6.591$ GHz. The reduced wake forces are, respectively, $\hat{F}_{z01} = 4.381$ for $m = 0$ and $\hat{F}'_{r11} = 1.464$ for $m = 1$. Using Eq. (2.1) multiplied by $Z_0 c/4\pi$ where $Z_0 = 377$ ohms to convert the force to mks units, we obtain the longitudinal acceleration gradient 3.943×10^{14} eV/m/C, or 39.4 MeV/m for a source bunch of 100 nC. Using Eq. (2.2), we obtain a transverse force of $1.32 \times 10^{16} r_0$ eV/m/C where r_0 is the offset of the source bunch from the axis of the waveguide expressed in m. The accelerating longitudinal force F_{01} (aside from the cosine factor) scales with a^{-2}, while the dipole transverse force F_{11} (aside from the sine factor) scales with a^{-3}. Therefore, increasing the outside radius of the waveguide will lower the transverse force by very much. Although not as fast, however, the accelerating force will be decreased also.

As a comparison, let us consider an iris-loaded waveguide having inner and outer iris radii $b = 5.11$ cm and $a = 10$ cm respectively. Numerical calculation[10] reveals a longitudinal field of frequency 1.15 GHz and a dipole traverse force of $1.2 \times 10^{14} r_0$(m) eV/m/C. For a dielectric waveguide of the same frequency, we need a guide radius of $a = 7.40$ cm provided that we keep $b/a = 0.2$ and $\epsilon = 3$. The dipole transverse wake force turns out to be $3.25 \times 10^{13} r_0$(m) eV/m/C, which is 3.7 times less than that of the iris-loaded waveguide. With suitable choices of parameters, it is possible that the dielectric-lined waveguide can have smaller deflecting wake forces than the iris-loaded waveguide.

VI. DISCUSSIONS

Simple analytic expressions for the reduced longitudinal and transverse forces have been derived in the limits when the dielectric lining is thin as well as thick. Numeri-

cal computation of the lowest modes have also been performed. We learn from these calculations that the reduced dipole transverse wake force has the same order of magnitude as the monopole longitudinal wake force except when the dielectric lining is very thin. This conclusion may not be in contradiction to what was observed experimentally in Ref. 6. This is because the deflecting wake force has never been actually measured there. In that experiment, the inner and outer radii of the three dielectric materials are, respectively, $b = 0.63$ cm and $a = 1.27$ cm. The three materials have dielectric constants $\epsilon \approx 3.1$, 5.9, and 3.9. According to our calculation, the deflecting force should be, respectively, $8.0 \times 10^{15} r_0(\mathrm{m})$ eV/m/C, $4.7 \times 10^{15} r_0(\mathrm{m})$ eV/m/C, and $6.8 \times 10^{15} r_0(\mathrm{m})$ eV/m/C.

The author would like to thank Drs. Wei Gai and Jim Rosenzweig for useful and encouraging discussions.

Note added in revision

During the writeup of this paper, the author was aware of similar work by other authors. Gluckstern[11] gave analytic expressions of the wake forces in the limit of a thin dielectric. Rosing[12] computed numerically the $m = 0$ longitudinal wake force.

REFERENCES

1. R.K. Keinigs, M.E. Jones, and W. Gai, Particle Accelerators **24**, 223 (1989).

2. C. Callen et al JASON report JSR-86-109, 1987.

3. A. Piwinski, DESY 72/72.

4. Y.Y. Lau, Phys. Rev. Lett. **63**,1141 (1989)

5. K.Y. Ng, Fermilab Report FN-533, 1990.

6. W. Gai et al Phys. Rev. Lett. **24**, 2756 (1988).

7. H. Figueroa et al, Phys. Rev. Lett. **60**, 2144 (1988).

8. J.B. Rosenzweig et al, Phys. Rev. Lett. **61**, 98 (1988).

9. W.K.H. Panofsky and W.A. Wenzel, Rev. Sci. Instrum. **27**, 967 (1965).

10. J.D. Simpson, *Proposal of the Argonne Wakefield Accelerator*, Argonne National Lab Report ANL-HEP-TR-89-81, 1989.

11. R.L. Gluckstern, LANL Report AT-6:ATN-90-1, 1990.

12. M. Rosing, Argonne Lab Report WF-126, 1989.

Figure Captions

Fig. 1. Lowest reduced eigen frequency of the $m = 0$ longitudinal mode.

Fig. 2. Lowest reduced eigen frequency of the $m = 1$ transverse mode.

Fig. 3. Ratio of lowest $m = 1$ eigen frequency to lowest $m = 0$ eigen frequency.

Fig. 4. Reduced $m = 0$ longitudinal force $\hat{F}_{z01}$ of the lowest mode.

Fig. 5. Reduced $m = 1$ transverse force $\hat{F}'_{r11}$ of the lowest mode.

Fig. 6. Ratio of transverse force to longitudinal force. $\hat{F}'_{r11}/\hat{F}_{z01}$. Both forces are of the lowest modes.

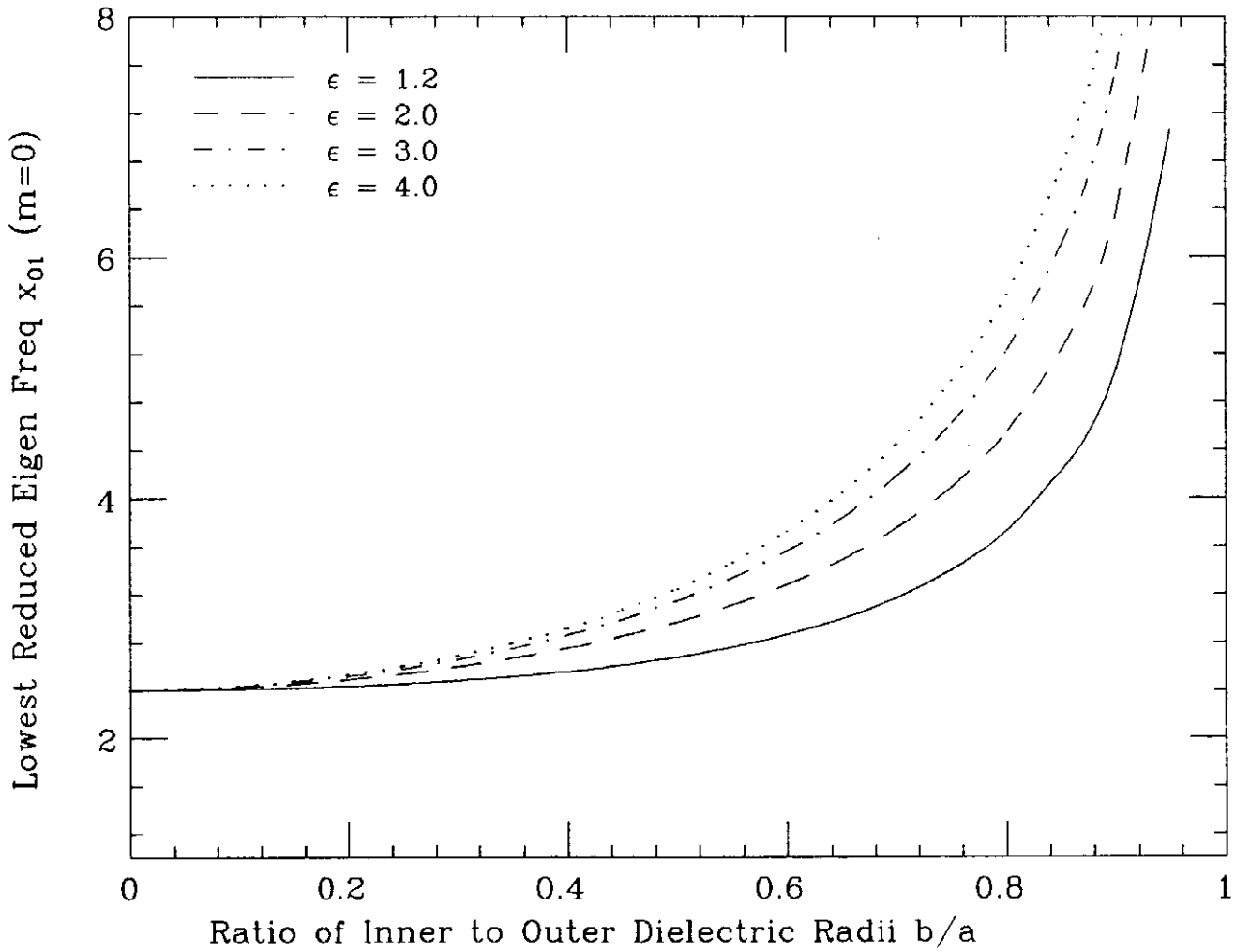
8
6
4
2
0
0.2
0.4
0.6
0.8
1
ε = 1.2
ε = 2.0
ε = 3.0
ε = 4.0
Lowest Reduced Eigen Freq x_{01} (m=0)
Ratio of Inner to Outer Dielectric Radii b/a

Figure 1

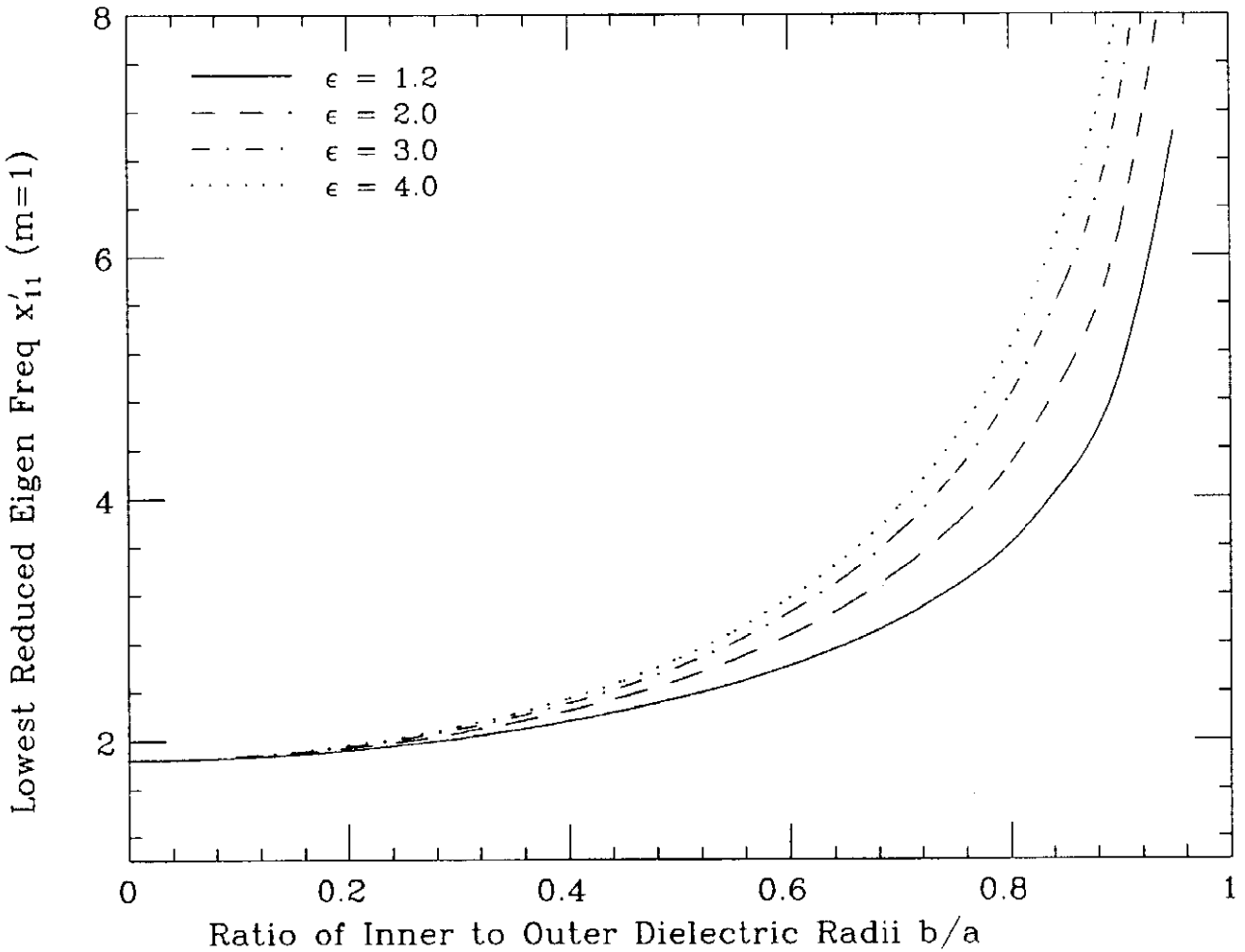
8
6
4
2
0
0.2
0.4
0.6
0.8
1
ϵ = 1.2
ϵ = 2.0
ϵ = 3.0
ϵ = 4.0
Lowest Reduced Eigen Freq x'_{11} (m=1)
Ratio of Inner to Outer Dielectric Radii b/a

Figure 2

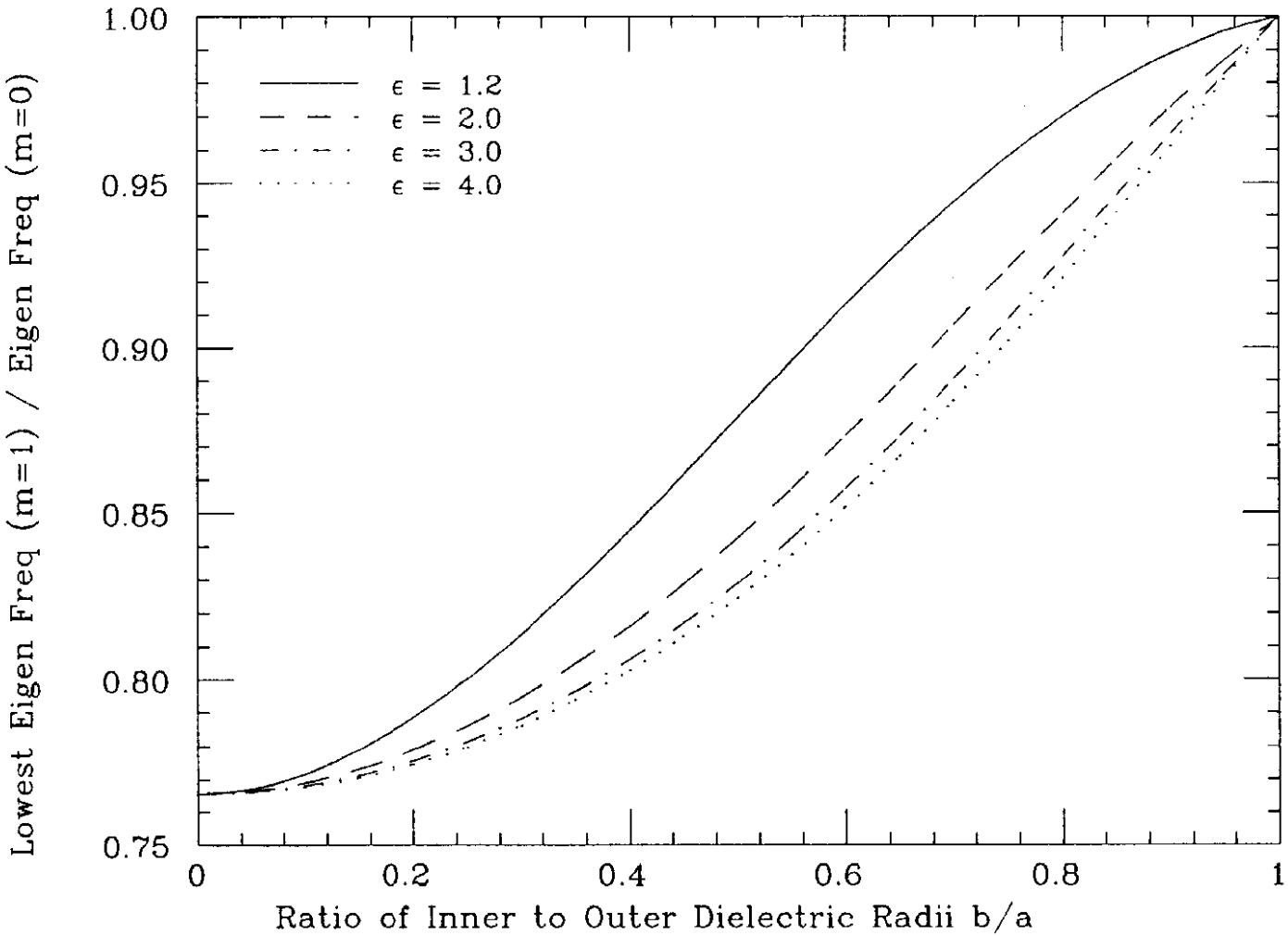
1.00
0.95
0.90
0.85
0.80
0.75
0
0.2
0.4
0.6
0.8
1
ϵ = 1.2
ϵ = 2.0
ϵ = 3.0
ϵ = 4.0
Lowest Eigen Freq (m=1) / Eigen Freq (m=0)
Ratio of Inner to Outer Dielectric Radii b/a

Figure 3

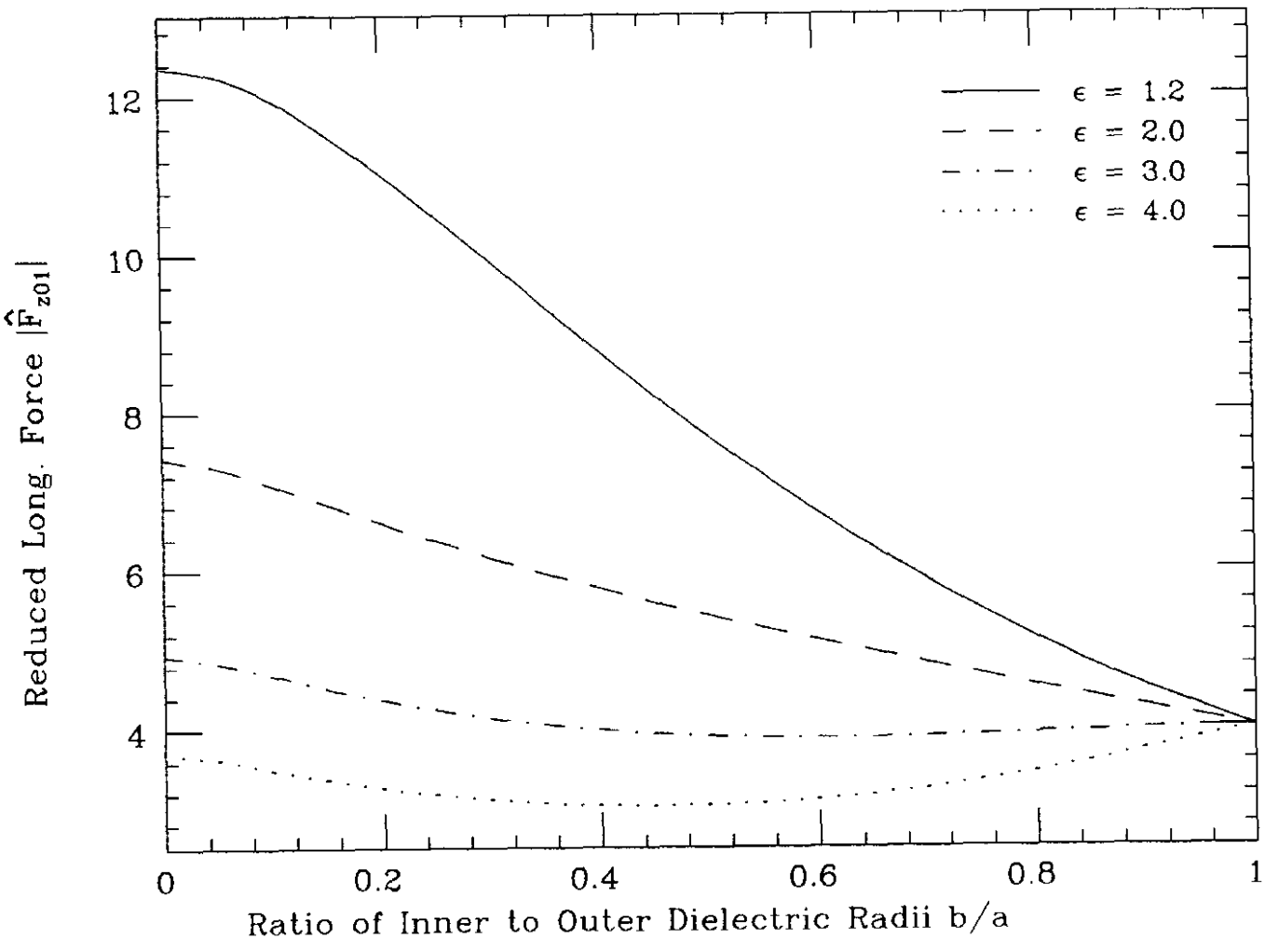
Reduced Long. Force $|\hat{F}_{z01}|$
12
10
8
6
4
0
0.2
0.4
0.6
0.8
1
Ratio of Inner to Outer Dielectric Radii b/a
ϵ = 1.2
ϵ = 2.0
ϵ = 3.0
ϵ = 4.0

Figure 4

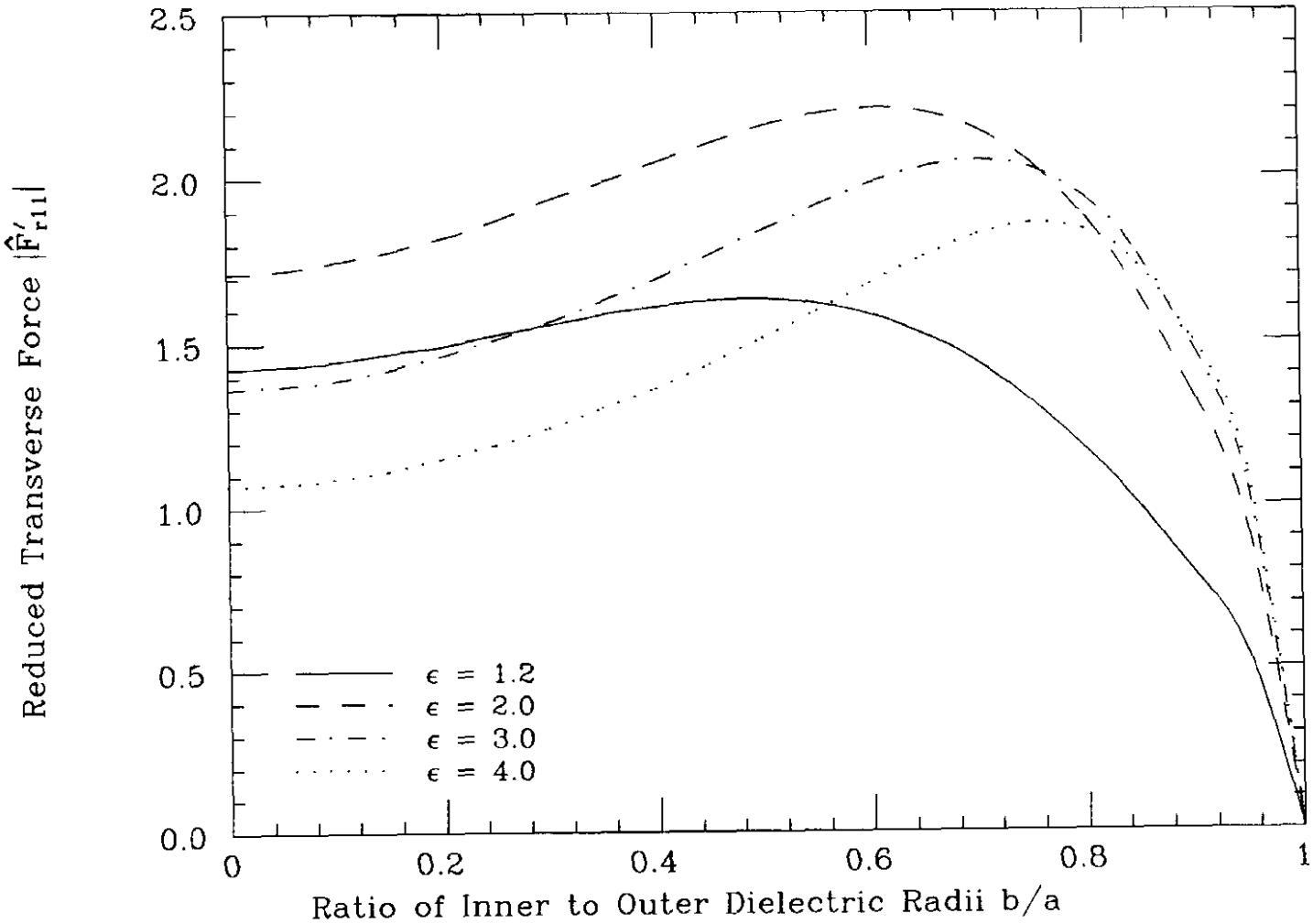
Reduced Transverse Force $|\hat{F}'_{r11}|$
2.5
2.0
1.5
1.0
0.5
0.0
0
0.2
0.4
0.6
0.8
1
ϵ = 1.2
ϵ = 2.0
ϵ = 3.0
ϵ = 4.0
Ratio of Inner to Outer Dielectric Radii b/a

Figure 5

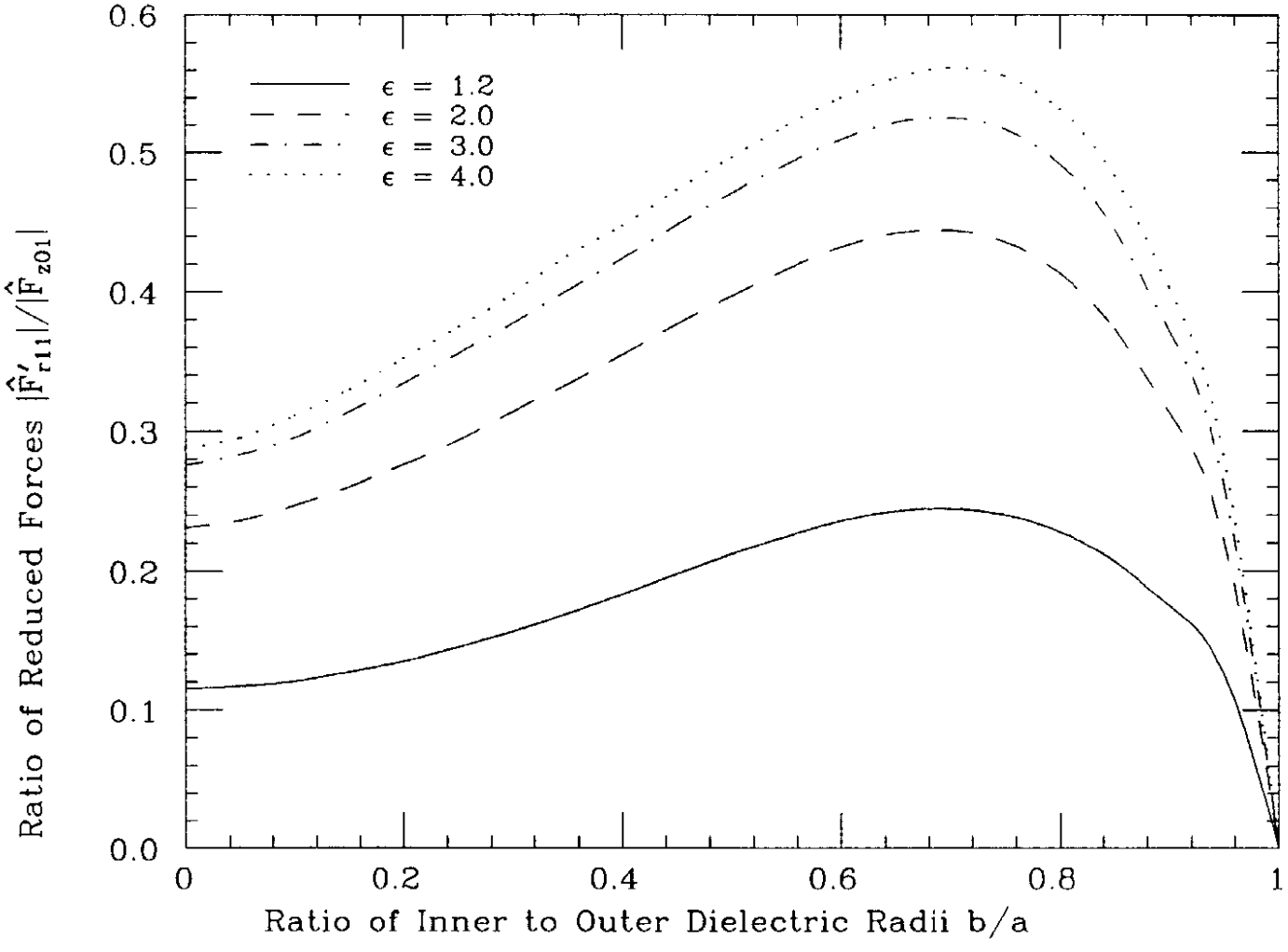
0.6
0.5
0.4
0.3
0.2
0.1
0.0
0
0.2
0.4
0.6
0.8
1
ϵ = 1.2
ϵ = 2.0
ϵ = 3.0
ϵ = 4.0
Ratio of Reduced Forces $|\hat{F}'_{r11}|/|\hat{F}_{z01}|$
Ratio of Inner to Outer Dielectric Radii b/a

Figure 6